



**CRISP Development Report**

**JOINT INTERFACE (SLIP) ELEMENTS IN CRISP  
IN 2D AND 3D SPACE**

Job no. **9801**  
CRISP release worked on: **CRISP-97**  
Resulting CRISP release worked for: **MP V98.9, GP V98.9**

Developer: **Amir Rahim**  
Date: **March 1998**

## 1. Summary

In this development work, a new effective stress interface element has been introduced in Crisp. This allows the interfacing of consolidating material with drained material. The effective normal stress is then used as the controlling parameter in the Mohr-Coulomb criterion used for the interface element. In addition the existing 'total stress' interface element has been modified to allow improved simulation of stiffness during cyclic shear loading as well as during re-bonding. Finally, a new 3D interface element has been introduced. This has two local shear stresses and one local normal stress.

## 2. Basic Theory of 2D Interface element

Goodman's interface element is currently used in CRISP to allow slip to occur between dissimilar materials or materials having a large difference in their stiffnesses. An example of this is the settlement of soil behind a concrete wall where the soil moves relative to the concrete. It is possible to use ordinary refined isoparametric elements with appropriate choice of stiffness, but the interface element allows the use of slender elements without the necessity to refine the mesh. The shear stress along the interface element is limited by the user specified interface shear strength. Mohr-Coulomb yield criterion is used to check whether the shear stress exceeded the maximum shear strength. If so, the residual shear modulus is then used in the calculation of element stiffness. Checks are made on whether the element has gone into tension. If so, both the normal stiffness and the shear stiffness are multiplied by a factor of 1/10000 so that the element can simulate separation.

The nodal coordinates for the 2D interface element are the same for the two rows of nodes along the length dimension of the element. The element thickness is specified as part of the material properties and this is used in the calculation of stiffness. The element geometry is shown below. In Crisp, the mid-side nodes on the shorter sides of the element are dummy nodes, and are there only to satisfy the geometry program. There are two degrees of freedom in the x and y direction for each node, except the dummy nodes which have no degrees of freedom.

The interface element is characterised by the normal and shear stresses. The normal stress,  $\sigma$ , and the shear stress  $\tau$ , are related by the constitutive equation to the normal and tangential strain as follows:

$$\begin{Bmatrix} \Delta \mathbf{s} \\ \Delta \mathbf{t} \end{Bmatrix} = [D] \begin{Bmatrix} \Delta \mathbf{e} \\ \Delta \mathbf{g} \end{Bmatrix} \quad \text{Eq. 1}$$

For plane strain condition, the [D] matrix takes the form:

$$[D] = \begin{bmatrix} k_n & 0 \\ 0 & k_s \end{bmatrix} \quad \text{Eq. 2}$$

where  $k_n$  and  $k_s$  are the elastic normal and shear stiffnesses.

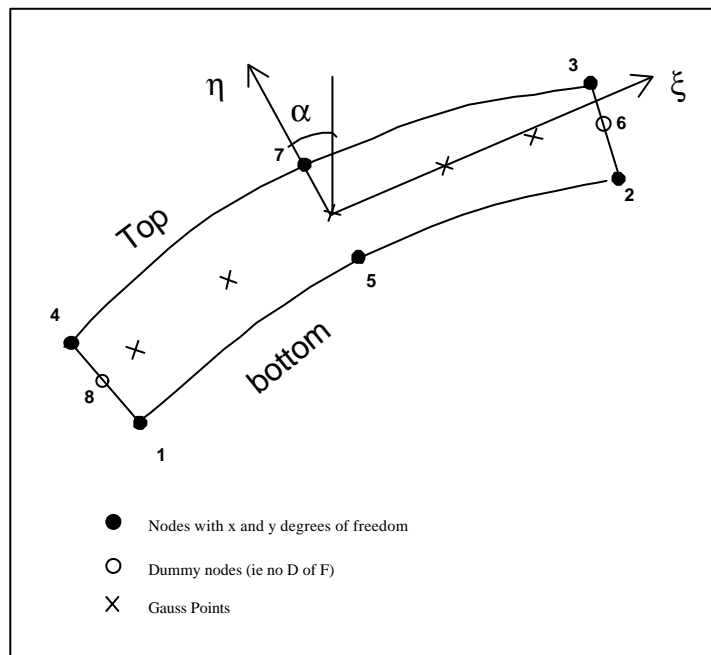


**Figure 1** Geometry of 2D interface element

The global coordinates at any point on the element are related to the nodal values using the shape functions,  $N_i$ , thus:

$$\begin{aligned}x^{bottom} &= N_1 x_1 + N_2 x_2 + N_5 x_5 \\x^{top} &= N_3 x_3 + N_4 x_4 + N_6 x_6 \\y^{bottom} &= N_1 y_1 + N_2 y_2 + N_5 y_5 \\y^{top} &= N_3 y_3 + N_4 y_4 + N_6 y_6\end{aligned}\tag{Eq. 3}$$

The global displacements at any point are expressed in terms of the nodal displacements using the same isoparametric shape functions as follows:

$$\begin{aligned}u^{bottom} &= N_1 u_1 + N_2 u_2 + N_5 u_5 \\u^{top} &= N_3 u_3 + N_4 u_4 + N_6 u_6 \\v^{bottom} &= N_1 v_1 + N_2 v_2 + N_5 v_5 \\v^{top} &= N_3 v_3 + N_4 v_4 + N_6 v_6\end{aligned}\tag{Eq. 4}$$

The isoparametric shape functions are defined as

$$N_1 = N_4 = \frac{1}{2} \mathbf{x}(\mathbf{x}-1) \quad N_2 = N_3 = \frac{1}{2} \mathbf{x}(\mathbf{x}+1) \quad N_5 = N_6 = (1-\mathbf{x}^2)$$

where  $\xi$  is the local coordinate which varies from -1 to +1 over the element length.

The displacements in the local coordinates system can now be defined as follows

$$\begin{Bmatrix} u_l \\ v_l \end{Bmatrix} = \begin{bmatrix} \cos \mathbf{a} & \sin \mathbf{a} \\ -\sin \mathbf{a} & \cos \mathbf{a} \end{bmatrix} \begin{Bmatrix} u \\ v \end{Bmatrix}\tag{Eq. 5}$$

The trigonometric values  $\sin(\alpha)$  and  $\cos(\alpha)$  may be found from the derivatives of the global coordinates w.r.t to the local coordinates, thus:

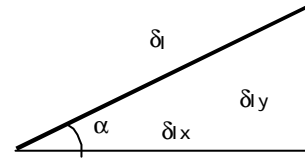


**Figure 2** Transformation of coordinates

Using the relationships:

$$\mathbf{d}_x = \frac{dx}{d\mathbf{x}} \mathbf{d}\mathbf{x} \quad \mathbf{d}_y = \frac{dy}{d\mathbf{x}} \mathbf{d}\mathbf{x}\tag{Eq. 6}$$

we have

$$\mathbf{d} = \sqrt{\left(\frac{dx}{d\mathbf{x}}\right)^2 + \left(\frac{dy}{d\mathbf{x}}\right)^2} d\mathbf{x}\tag{Eq. 7}$$

The derivatives of the global coordinates w.r.t. the local axes are:

$$\begin{aligned}\frac{dx}{d\mathbf{x}} &= \frac{dN_1}{d\mathbf{x}} x_1 + \frac{dN_2}{d\mathbf{x}} x_2 + \frac{dN_5}{d\mathbf{x}} x_5 \\ \frac{dy}{d\mathbf{x}} &= \frac{dN_1}{d\mathbf{x}} y_1 + \frac{dN_2}{d\mathbf{x}} y_2 + \frac{dN_5}{d\mathbf{x}} y_5\end{aligned}\tag{Eq. 8}$$

The trigonometric functions  $\sin(\alpha)$  and  $\cos(\alpha)$  can now be defined as

$$\sin \mathbf{a} = \frac{1}{|J|} \frac{dy}{d\mathbf{x}} \quad \cos \mathbf{a} = \frac{1}{|J|} \frac{dx}{d\mathbf{x}} \quad \text{Eq. 9}$$

where  $|J|$  is

$$|J| = \left[ \left( \frac{dx}{d\mathbf{x}} \right)^2 + \left( \frac{dy}{d\mathbf{x}} \right)^2 \right]^{1/2} \quad \text{Eq. 10}$$

The incremental strains may now be obtained in a new form, thus:

$$\begin{Bmatrix} \Delta \mathbf{e} \\ \Delta \mathbf{g} \end{Bmatrix} = [B] \{a_e\} \quad \text{Eq. 11}$$

where  $a_e$  is a vector listing all the nodal displacements in the element, ie

$$a_e = \{u_1 \ v_1 \ u_2 \ v_2 \ u_3 \ v_3 \ u_4 \ v_4 \ u_5 \ v_5 \ u_6 \ v_6\} \quad \text{Eq. 12}$$

The matrix  $B$  contains the derivatives of the shape functions w.r.t to the global axes. In order to obtain that, we must first find  $B_{local}$  which contains the derivatives of the shape functions w.r.t to the local axis  $\xi$ . This is expressed as follows:

$$B_{local} = \begin{bmatrix} 0 & N'_1 & 0 & N'_2 & 0 & -N'_3 & 0 & -N'_4 & 0 & N'_5 & 0 & -N'_7 \\ N'_1 & 0 & N'_2 & 0 & -N'_3 & 0 & -N'_4 & 0 & N'_5 & 0 & -N'_7 & 0 \end{bmatrix} \quad \text{Eq. 13}$$

$$\text{where } N'_i = \frac{dN_i}{d\mathbf{x}} = \frac{N_i}{\text{thickness}}$$

The element thickness is specified as a material parameter (see table bellow).

Transforming to the global coordinates system we get,

$$B = \begin{bmatrix} \cos \mathbf{a} & -\sin \mathbf{a} \\ \sin \mathbf{a} & \cos \mathbf{a} \end{bmatrix} [B_{local}] \quad \text{Eq. 14}$$

The determinant of the Jacobian matrix  $|J|$  as defined in equation (9) is also used in transformed integrals as follows:

$$\int \int dx dy = \int_{-1}^1 |J| d\mathbf{x}$$

The element stiffness matrix is evaluated using local coordinates system, thus:

$$[K_e] = \int_{-1}^1 [B]^T [D][B] |J| d\mathbf{x} \quad \text{Eq. 15}$$

Once the displacements are found, incremental strains are calculated using equation 8, then incremental stresses are found using equation 1. The normal stress  $\sigma$  is then updated, and the limiting shear stress is evaluated using Mohr Coulomb yield criterion as follows:

$$\mathbf{t}_{limit} = C + \mathbf{s} \tan(\mathbf{f}) \quad \text{Eq. 16}$$

where  $C$  and  $\phi$  are the cohesion and angle of internal friction respectively.

If  $\tau$  is found to have exceeded  $\tau_{limit}$  then, the shear stiffness  $K_s$  is replaced by the residual shear stiffness  $K_{sres}$ . In addition, a further check is made on the normal stress. If  $\sigma$  is found to be negative which indicates that tension has occurred, then both the normal and shear stiffnesses are set to a very small value by multiplying  $K_s$  and  $K_n$  by a factor of 1/10000.

### 3. 2D 'effective stress' interface element

This is the same as that of the traditional 'total stress' interface element, except that the new element allows for the presence of two pore pressure nodes on one side. These nodes may have three degrees of freedom in x and y direction as well as a pore pressure degree of freedom.

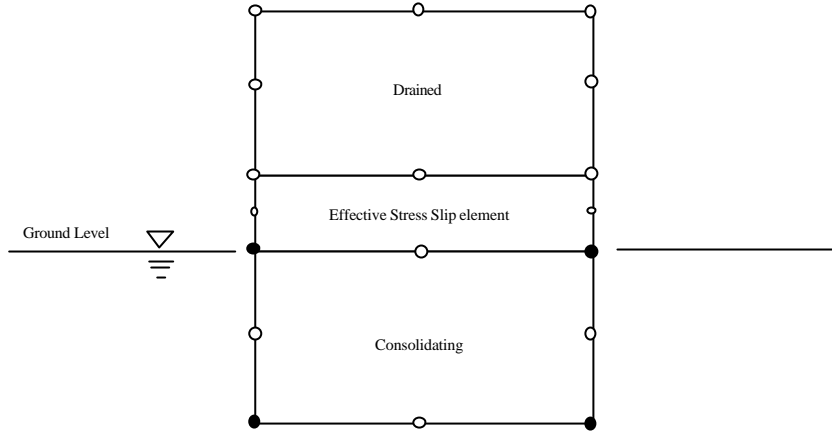


**Figure 3** Geometry of 2D 'Effective Stress' interface element

Stiffness assembly is the same as for the usual 'total stress' interface element. The new changes were restricted to the stress evaluation stage. Here, the pore pressure is calculated at each Gauss point as follows:

$$\overline{\Delta u} = \overline{N} \Delta \mathbf{b} \tag{Eq. 17}$$

where  $\overline{N}$  represents the shape functions of the two pore pressure nodes on one side of the interface element, and  $\Delta \mathbf{b}$  is a vector of excess pore pressure for these two nodes. The excess pore pressure variables belong to the neighbouring consolidation element, therefore a search is made to identify the adjacent consolidation element before this step is carried out.

The normal and shear stresses are calculated as usual without the pore pressure. The effective normal stress is used in the Mohr-Coulomb yield criterion to check whether the shear stress has exceeded the shear strength. Pore pressure is then added to the normal stresses if interface element is in compression so that correct normal forces can be calculated.

#### 4. New interface element for 3D space

This is similar to the 20-noded 'brick' element, except that the nodal coordinates are the same in the upper side as the corresponding nodes in the lower sides. The element is planar in the x-z plane and the thickness (or height) is specified within the element properties. The element has 3x3 Gauss integration points in the x-z plane.

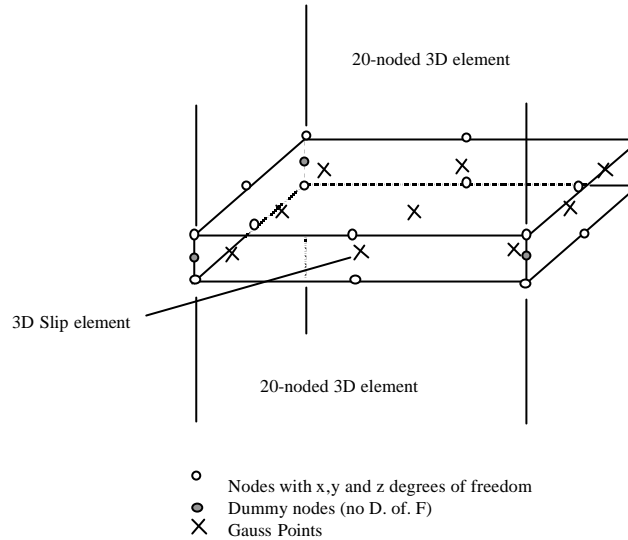


**Figure 4** Geometry of 3D interface element

The coding for this element has been provided by Professor Mike Gunn, and is now implemented in Crisp 98. Element details were provided in the module BLOCK DATA. This element has some similarity with the 20-noded brick element, though it has only 3x3 Gauss points in the x-z plane as can be seen in the element geometry above.

New subroutines were introduced for this special element. These are:

- FOSL3D      Calculates the force matrix equivalent to element stresses. This assumes an 8-noded element with 3x3 Gauss points in the x-z plane.
- LSLP3D      Calculates element stiffness again assuming an 8-noded element with 3x3 Gauss points in x-z plane
- SHPE3D      Calculates element shape functions assuming 8-noded element in x-z plane
- OUTS3D      Calculates incremental stresses and their equivalent nodal forces
- DSL3D      Assembles D matrix and adjusts components if tension or shear stress limit is reached. Called by OUTS3D

Changes were needed in the following routines:

- EQVFOR              calls FOSL3D
- INSIT                calls SHPE3D
- FRONTZ and FRONTU    calls LSLP3D
- UPOUT                calls OUTS3D

Special coding was also added to routine INSIT so that the 3D interface element appears as an 8-noded element in the x-z plane. This is necessary so that correct in-situ stresses can be calculated.

## 5. Interface element properties

All of the three elements featured above have the same set of properties as follows:

<b>Symbol</b>	<b>Property</b>	<b>Units</b>
c	cohesion intercept	force/unit area
$\phi$	angle of friction	degrees
$K_n$	Stiffness modulus of normal direction	force /unit area
$K_s$	Shear modulus	force /unit area
$K_{sres}$	Residual shear modulus	force /unit area
t	element thickness	unit length

## 6. Improvements of the existing 2D 'total stress' interface element

The element must be able to model deformation behaviour in the normal direction as well as the shear direction. These modes of behaviour were presented by C.F NG et.al [1] and are shown as follows:

**Figure 5 Expected behaviour in normal direction**

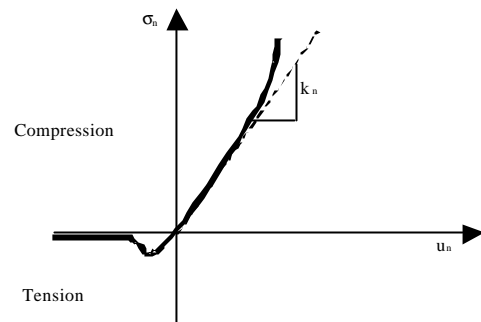
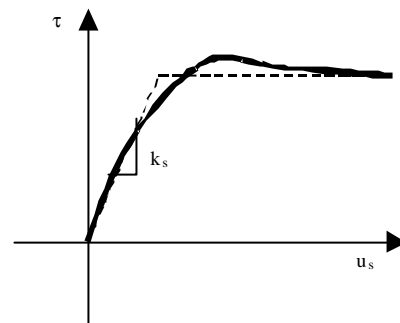


**Figure 6 Expected behaviour in shear direction**



During loading, unloading and re-loading, the element is expected to make use of the appropriate shear and normal stiffness as represented in the following figures:

**Figure 7 Modes of normal deformation behaviour**

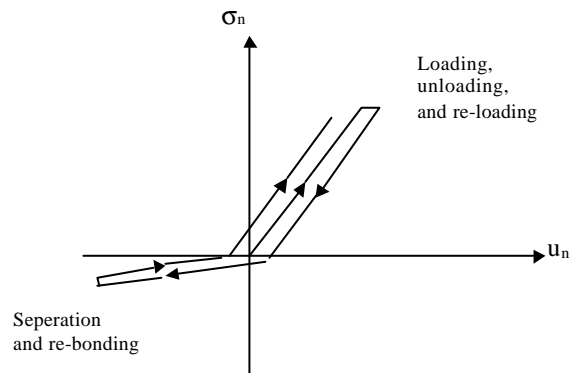
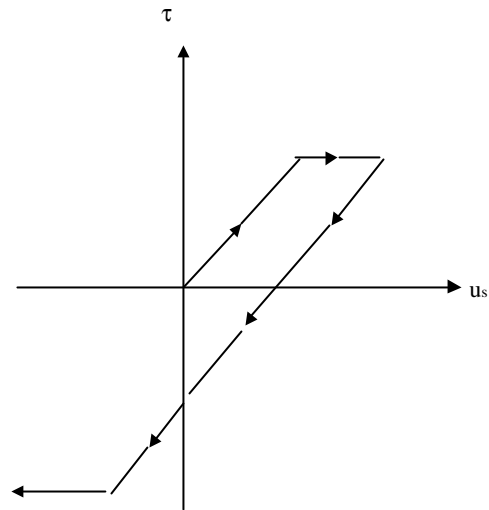




**Figure 8 modes of shear deformation behaviour**



### 6.1. Single Element Tests

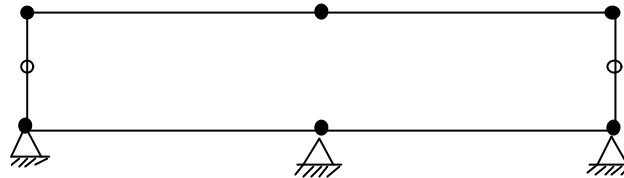


**Figure 9 single interface element**

A single element of unit length is assembled as shown in Figure 9

The loading consists of prescribed horizontal and vertical displacements applied to the top edge

The properties chosen are as follows:

$$c=30 \quad \phi=30 \quad k_n=1000,000 \quad k_s=375,000 \quad K_{sres}=100 \quad t=0.1$$

The stiffness moduli  $k_n$  and  $k_s$  are defined from the relationships

$$K_n = k_n \times t = \frac{E(1-\mathbf{u})}{(1+\mathbf{n})(1-2\mathbf{u})} \quad K_s = k_s \times t = \frac{E}{2(1+\mathbf{u})}$$

It is worth noting that the performance of the element is not sensitive to the thickness ( $t$ ). Similar results may be obtained if the ratios  $K_n/t$  and  $K_s/t$  are kept constants

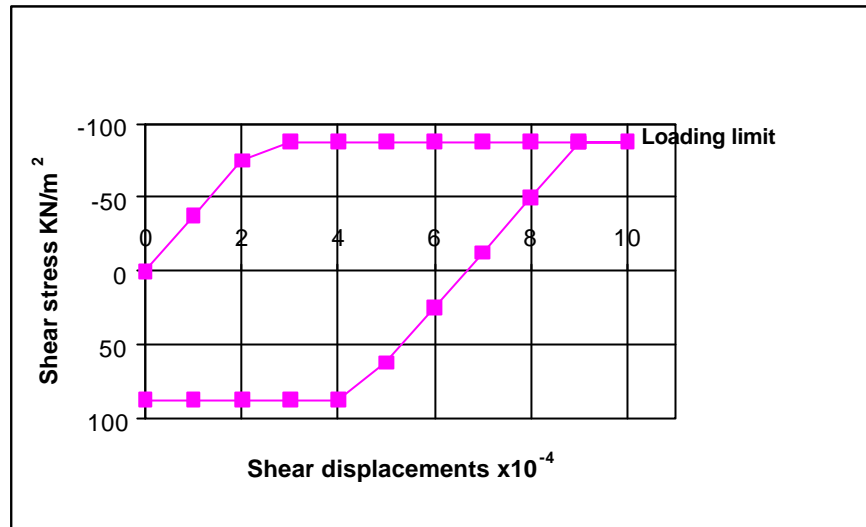
#### (i) Testing for Shear stress behaviour

The residual shear modulus  $K_{sres}$  defines the shear stiffness after reaching the limiting shear stress  $\tau_{lim}$ . Within CRISP, the shear modulus  $K_s$  is changed to  $K_{sres}$  in subroutine DSLIP when the shear stress reaches  $0.99 \tau_{lim}$ . As will be explained later, the limiting value of  $0.99$  was found to be inappropriate for capturing unloading and had to be increased to  $0.99999$ .

For this test, a pressure load of  $100$  was applied initially to ensure that the element remains in contact during shear. A displacement of  $1 \times 10^{-3}$  was first applied in  $10$  increments. This was followed by a negative displacement of  $-1 \times 10^{-3}$  applied in another  $10$  increments. Using CRISP97, the results were similar to those shown above up to the point labelled 'loading limit'. For the load reversal stage, (displacements applied in negative  $x$ -direction) CRISP97 produced erroneous results in which the shear stress remained at the limiting value. The reason for this was found to be the limiting value of  $0.99 \tau_{lim}$ . Incremental stresses produced in the load reversal stage were very small as  $K_{sres}$  is now used. Thus the

appropriate shear stiffness ( $K_s$ ) was not invoked in the unloading stage. The limit of  $0.99 \tau_{lim}$  was then increased to  $0.99999 \tau_{lim}$ . This produced correct results as indicated in the graph above. One may notice the lag in the graph just after the loading limit.

Figure 10



(ii) Testing for Normal Stress behaviour

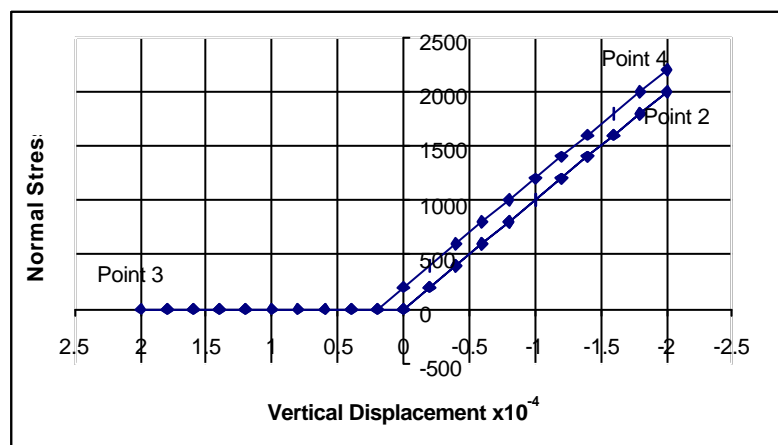
For this test a vertical downward displacement of  $-0.0002$  was applied along the top edge for the first 10 increments. This was followed by an applied upward displacement of  $0.0004$ , followed by a reversed downward displacement of  $0.0004$ .

Using CRISP97, the normal stress deformation profile was represented correctly for the loading stage up to point 2 and for the unloading stage up to point 3 which is in the separation zone. CRISP97 sets the stresses in the tensile region to a low value once the stresses are found to be negative.

In the re-bonding (re-contact) stage from point 3 to point 4, CRISP97 produced incorrect results as the Normal modulus  $K_n$  was immediately activated at point 3. This meant that the normal stiffness is activated at the start of the rebonding stage even though the element's gap is not yet closed.

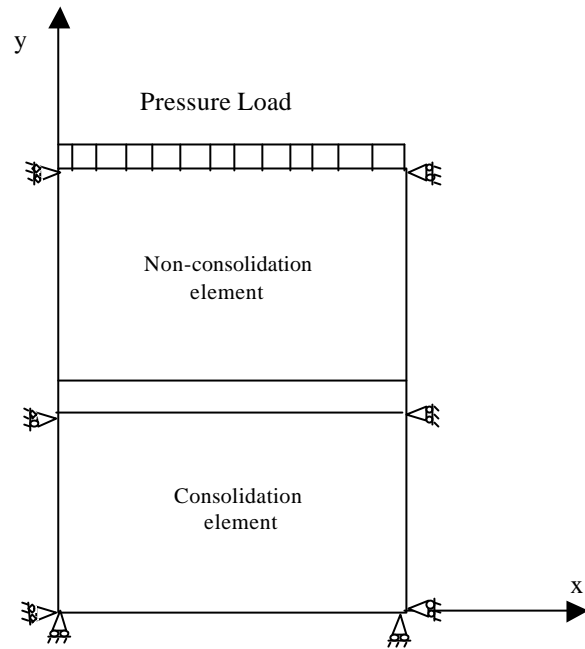
To solve this problem, a simple flag system was introduced. This is coded in routine OUTSLP. Once the normal stress becomes negative (ie tensile), the flag is set to 1. This flag is stored in the stress array `varint(3,igp,ielem)` which is unused for the interface element. Subsequently, in the stiffness evaluation stage of the next increment, if the flag is found to be equal to 1, a factor of 10000 is used to reduced the stiffness moduli  $K_n$  and  $K_s$ . This reduced stiffness allows appropriate modelling of re-bonding in which the usual moduli of  $K_n$  and  $K_s$  are only used when the gap is closed. If the normal stress is found to be compressive during re-bonding, the flag is set to zero and the usual stiffness moduli are then used.

Figure 11

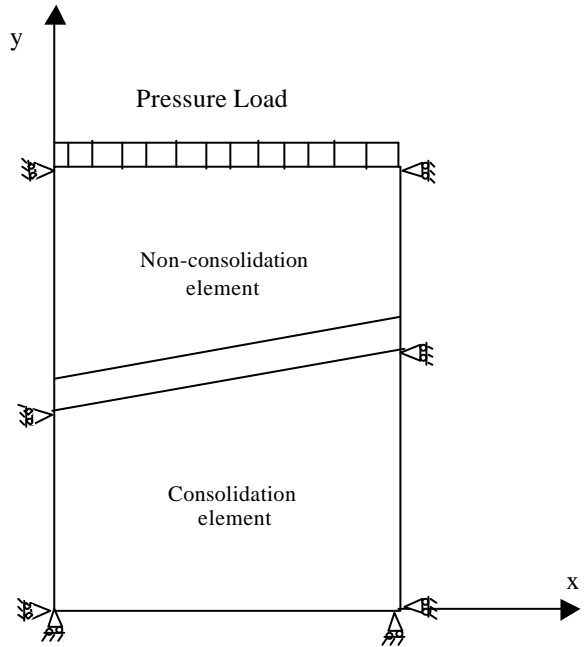


## 7. Validation of new 'Effective Stress' interface element

Test 1



Test 2

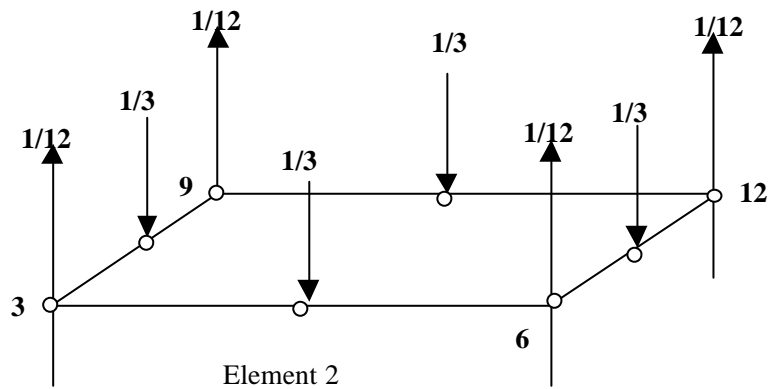
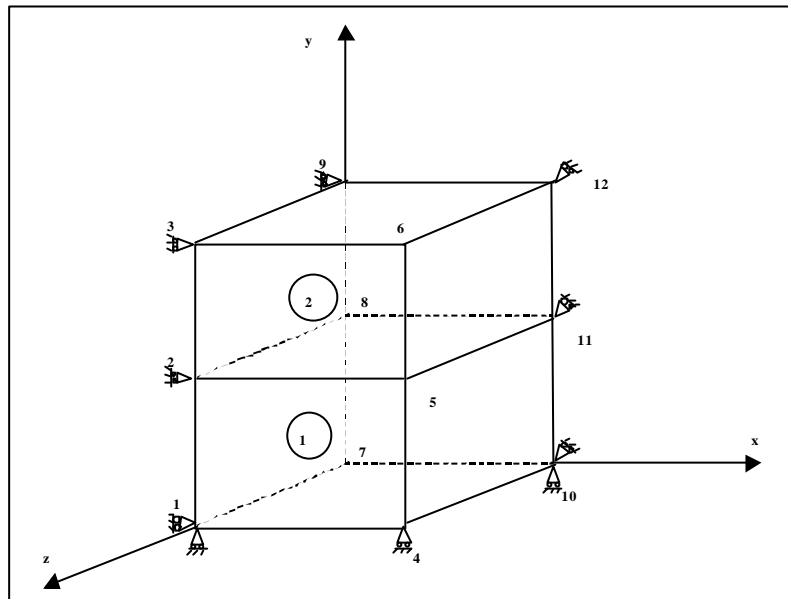


## 8. Validation of new 3D interface element

A simple mesh of two brick elements was assembled. Several tests were conducted by attaching a 3D interface element between the two brick elements. The purpose is to find the distribution of stresses within the slip element.

### Test 1

For this test only two brick elements were used as shown. Point loads representing a uniform pressure were applied to the top surface. Nodal distribution of pressure load for 3D 20-noded element is shown in figure () below. The purpose of this test is to find the distribution of vertical stresses in both elements which was found to be equivalent to the applied uniform load



### Test 2.

Using the same mesh above, a single 3D interface element was inserted between element 1 and 2. The same boundary conditions and pressure loading were used. It was found that the normal stress within the interface element is exactly the same as the vertical stress in element 1 and 2 which in turn is the same as the applied pressure.

Test 3

